Received: 10 January 2020 | Revised: 29 May 2020 | Accepted: 8 June 2020

DOI: 10.1111/all.14519

ORIGINAL ARTICLE

Atopic Dermatitis, Urticaria and Skin Disease

Integrative transcriptome analysis deciphers mechanisms of nickel contact dermatitis

Lukas Wisgrill[1,2] | Paulina Werner[2] | Erja Jalonen[3] | Angelika Berger[1] | Antti Lauerma[3] | Harri Alenius[2,4] | Nanna Fyhrquist[2,4]

[1]Division of Neonatology, Pediatric Intensive Care and Neuropediatrics, Comprehensive Center for Pediatrics, Medical University of Vienna, Vienna, Austria

[2]Institute of Environmental Medicine, Karolinska Institutet, Stockholm, Sweden

[3]Skin and Allergy Hospital, Helsinki University Hospital, Helsinki, Finland

[4]Human Microbiome Program (HUMI), Medicum, University of Helsinki, Helsinki, Finland

Correspondence
Nanna Fyhrquist, Karolinska Institutet, Institute of Environmental Medicine (IMM), Box 210, 171 77 Stockholm, Sweden.
Email: nanna.fyhrquist@ki.se

Funding information
This research has received funding from the Finnish Work Environment Fund (project nr 113314) and Forskningsrådet för hälsa, arbetsliv och välfärd (FORTE, diarienr. 2018-00601).

Abstract

Background: Nickel-induced allergic contact dermatitis (nACD) remains a major occupational skin disorder, significantly impacting the quality of life of suffering patients. Complex cellular compositional changes and associated immunological pathways are partly resolved in humans; thus, the impact of nACD on human skin needs to be further elucidated.

Methods: To decipher involved immunological players and pathways, human skin biopsies were taken at 0, 2, 48, and 96 hours after nickel patch test in six nickel-allergic patients. Gene expression profiles were analyzed via microarray.

Results: Leukocyte deconvolution of nACD-affected skin identified major leukocyte compositional changes at 48 and 96 hours, including natural killer (NK) cells, macrophage polarization, and T-cell immunity. Gene set enrichment analysis mirrored cellular-linked functional pathways enriched over time. NK cell infiltration and cytotoxic pathways were uniquely found in nACD-affected skin compared to sodium lauryl sulfate–induced irritant skin reactions.

Conclusion: These results highlight key immunological leukocyte subsets as well as associated pathways in nACD, providing insights into pathophysiology with the potential to unravel novel therapeutic targets.

KEYWORDS

contact dermatitis, nickel, transcriptomics

1 | INTRODUCTION

Nickel is the leading contact allergen in industrialized countries displaying a tremendous impact on socioeconomics as well as quality of life of suffering patients.[1,2] The prevalence lies between 8% and 19% in adults, and 8% and 10% in children and adolescents, with a strong bias toward female gender.[3-6] Despite attempts to restrict the use of nickel, it is widely used in various products including metallic items, household products, and cosmetics due to its beneficial elemental properties and low cost.[2,7-10] Therefore, nickel skin contact avoidance in everyday life is hard to accomplish.

Nickel contact allergy is a cell-mediated type IV hypersensitivity reaction, involving both innate and adaptive immune mechanisms. In the multifarious cellular system of the human skin, different complex pathways and interwoven networks are activated during nickel-induced allergic contact dermatitis (nACD).[11-13]

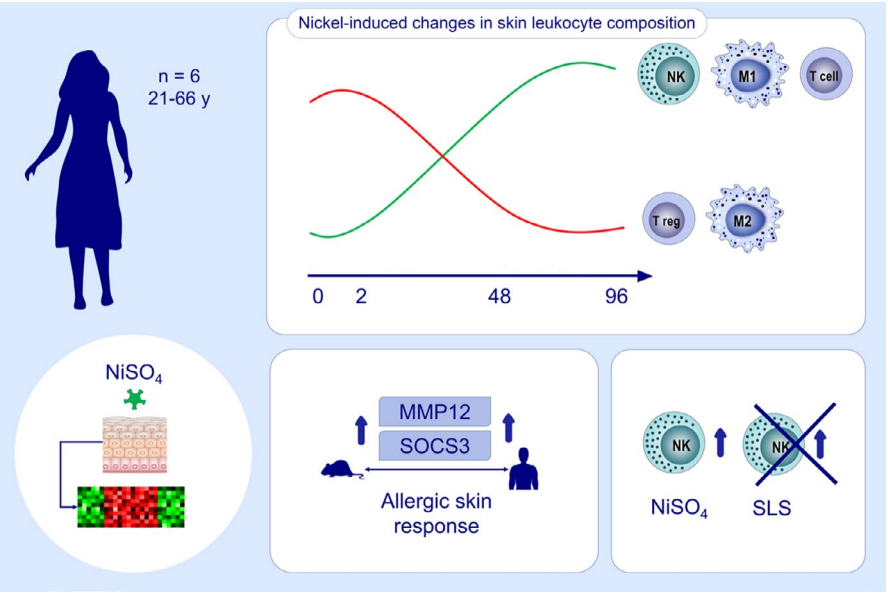

GRAPHICAL ABSTRACT

Late-phase nickel challenge induces major changes in leukocyte composition including influx and activation of NK cells, macrophage polarization, and T-cell immunity. *MMP12* and *SOCS3* are highly upregulated, linking our human findings to previous findings in mice. NK cell infiltration and cytotoxic pathways were found to be uniquely upregulated in nickel-induced allergic skin responses compared to SLS-induced irritant skin responses.

Abbreviations: MMP12, matrix metallopeptidase 12; $NiSO_4$, nickel sulfate; SLS, sodium lauryl sulfate; SOCS3, suppressor of cytokine signaling 3

Various studies derived from mice and human investigated diverse cellular subsets and mechanisms to illuminate central pathways in allergic contact dermatitis (ACD). Although the sensitization phase is extensively characterized,[11,14] immunological events during the elicitation phase, including cellular immune subsets as well as underlying mechanisms and cellular pathways, are not completely elucidated.

To decipher immune cell involvement and immunological pathways in more detail, we conducted time-course transcriptome experiments in nickel-allergic patients assessing gene expression profile changes during nickel patch tests. Thus, we aim to unravel novel pathomechanistical insights into nACD in the context of temporal dynamics of cell in- and efflux.

2 | METHODS

2.1 | Patient recruitment and sample collection

Patients over 18 years of age were recruited at the University of Helsinki at the Finnish Institute of Occupational Health. The study was approved by the Ethics Committee of Medicine, Helsinki University Central Hospital (§214/3.9.2014, dnro 171/13/03/01/20214), and all patients gave written informed consent prior to study inclusion. The patient selection was based on clinical history as well as patch test results over time. Only patients with a full ACD reaction at 96 hours were included in the study. Patch test reactions against sodium lauryl sulfate (SLS) were taken from the same patients. Exclusion criteria included large or disseminated eczema or other skin disorders. Application of topical medications and emollients as well as bathing was avoided 24 hours before the study start. Reaction strengths are summarized in Table 1.

Patch tests were performed on the back of the patients, containing 5% NiSO4 (petrolatum as vehicle) and 1% SLS (aqua as vehicle). Biopsies (one test chamber per biopsy—8 mm diameter) were taken at 0, 2, 48, and 96 hours after nickel challenge, and 48 hours after SLS application. The 0-hour time point represents untouched skin without any application of allergens or irritants. A 3-mm punch biopsy was taken at the corresponding time point. The biopsy was immersed in RNAlater liquid (Thermo Fisher Scientific) and stored at −80°C until further analysis.

2.2 | RNA preparation and microarray analysis

RNA was extracted from the patient skin biopsies stored in RNAlater solution using the AllPrep DNA/RNA Mini Kit (Qiagen). The purity of RNA was analyzed by NanoDrop ND-1000 (Thermo Fisher Scientific), where a ratio of A260/A280 > 1.8 was considered pure. 300 ng of RNA was reverse-transcribed into cDNA and labeled with fluorescent color for analysis by DNA microarrays (SurePrint G3 Human Gene Expression Microarrays, Agilent). After hybridization of the fluorescence-labeled targets to the microarrays, a fluorescence image of the array was scanned, and fluorescence image data were generated. The fluorescence image was converted into expression level values for each probe on the array.

TABLE 1 Reaction strength to nickel and SLS exposure after removal of the patch test

Exposure	?+	+	++	+++	IR
SLS (48 h)	3	n/a	n/a	n/a	3
Nickel (48 h)	3	1	2	—	n/a
Nickel (96 h)	—	1	4	1	n/a

Note: ?+, uncertain reaction; +, weak allergic reaction; ++, moderate allergic reaction; +++, strong allergic reaction; IR, irritant reaction; n/a, not applicable.

Data preprocessing and differential expression analysis of the gene expression data were done in eUTOPIA.[15] Probe profile expression data were normalized using quantile normalization and corrected for batch processing effects using ComBat.[16] After mapping from probe sets to gene symbols, a differentially expressed gene (DEG) list was identified for each time point using limma.[17] DEGs were defined as a fold change ± 1.5 and a *P*-value <0.05 after adjustment for multiple comparisons (Benjamini-Hochberg). Data can be accessed via ArrayExpress database under the accession number: E-MTAB-8945.

2.3 | Leukocyte deconvolution analysis

The CIBERSORT algorithm was used to estimate the leukocyte subset proportions of 22 individual immune cells utilizing the "L22" validated gene signature matrix.[18] Estimations are based on 1000 permutations. No significance filter has been applied to the estimated cell fractions to include all samples for further analysis.

2.4 | Gene set enrichment analysis and network analysis

Gene set enrichment analysis (GSEA) was performed with software version 4.0.1.[19,20] GO Biological Processes and Reactome gene sets were downloaded from "Molecular Signature Databases v7.0" from the Broad Institute (http://software.broadinstitute.org/gsea/msigdb). GSEA preranked analysis was performed using default settings with optimized time-course parameter (collapse dataset = FALSE, permutation type = gene_set, metric for ranking genes = Pearson). Highly significant gene sets ($P < 0.01$ and FDR < 0.01) were visualized using the EnrichmentMap plug-in (v3.2)[21] for Cytoscape (v3.7.2).[22] Modules with ≥3 nodes and normalized enrichment scores (NES) >2 and <−2 were included in the final visualization. Modules were manually labeled using the WordCloud plug-in[23] for Cytoscape.[22] An interactive network map can be accessed via CyNetShare (www.cynetshare.ucsd.edu; URL: https://gist.githubusercontent.com/lukaswisgrill/21d51fd8bdff0de49133d203daebd3d3/raw/6abf9ed7aa8958fe5309b4f359c413772daa0398/nickel_time_course).

2.5 | Enrichment analysis and gene expression data visualization

Further data analysis and graph visualization were conducted using R software (v3.6.1, R Core Team 2019) with the ggplot2,[24] ggpubr,[25] and ggfortify[26] package for R. Venn diagrams were generated using the VennDiagram[27] package. Enrichment analysis of DEGs was performed using the clusterProfiler[28] and ReactomePA[29] R package. KEGG pathway illustrations were generated with the pathView[30] package for R.

2.6 | qPCR validation

Validation of the array results was performed by real-time qPCR. To this end, some of the samples from patients exposed to nickel for 48 hours (n = 4) and 96 hours (n = 5), and healthy skin (n = 4) were used for technical validation of the results. In addition, samples of an independent group of patients exposed to nickel for 48 hours (n = 4) and baseline control (n = 3) were included for biological validation of the results. In brief, a sample input of 300 ng RNA from skin biopsies was reverse-transcribed into cDNA using the High Capacity cDNA Reverse Transcription Kit (Life Science Technologies) in 25 μL per reaction. The thermocycler program for cDNA consisted of a start cycle at 25°C for 20 minutes followed by one cycle at 37°C for 120 minutes. Levels of *MMP12*, *SOCS3*, *ARG1*, and *NOS2* were analyzed by quantitative RT-PCR using TaqMan chemistry and the 7500 Fast Real-Time PCR System (Applied Biosystems). The thermocycler program used consisted of one cycle at 50°C for 2 minutes, one cycle at 95°C for 30 seconds followed by 40 cycles at 95°C for 3 seconds and at 60°C for 30 seconds. PCR amplification of the endogenous *GAPDH* for human targets was performed for each sample as a loading control and for normalization between samples. Primers and probes were purchased from Applied Biosystems. The results are expressed as relative units, which were obtained by calculations using the comparative CT method.

2.7 | Immunohistochemistry

To detect the number of macrophages and CD8+T cells, immunohistochemistry was performed. Paraffin-embedded, 3-μm-thick skin tissue sections were stained for CD68 (1:100, clone PG-M1, Dako, M087629-2) and CD8alpha (1:150, clone 144B, Abcam, ab17147) using the Mouse specific HRP/DAB Detection IHC Kit (Ab64259, Abcam), according to the manufacturer's protocol. In brief, after deparaffinization, tissue sections were blocked for endogenous peroxidases using hydrogen peroxide for 10 minutes. Antigen retrieval was performed by HIER (microwave in TE buffer pH 8.0), and blockage of unspecific binding was done by incubating sections with protein block for 10 minutes. Between each step, buffer washes using TBST (5 mmol/L Tris-HCl (pH 7.6), 150 mmol/L NaCl, and 0.1% (v/v) Tween-20) were interposed. Incubation with primary antibody was

done overnight (12-14 hours) at 4°C. After washing, the sections were incubated with secondary antibody for 10 minutes. The reactions were visualized with DAB and counterstained with Mayer's Htx (Dako).

2.8 | Digitalization of samples and image analysis

The stained skin biopsy slides were digitalized with a whole-slide scanner (Zeiss Axio Scan.Z1, ZEISS Microscopy) equipped with a 40X objective (numerical aperture 0.95) and camera set consisting of Hitachi HV-F203 f with an 1X adapter with 1600 × 1200 pixels sized 4.4 × 4.4 μm, resulting in an image in which one pixel represents an area of 0.11 μm × 0.11 μm. Images were stored in a whole-slide image format (CZI., ZEISS Microscopy), and compression of the files was performed using JPEG XR with a quality setting of 85% in ZEN Blue v.3.1 (ZEISS Microscopy). The compressed images were then uploaded to the whole-slide image management server Aiforia (Aiforia Technologies Oy). The proportion of positive cells were counted manually in five randomly selected areas (4000 × 4000 pixels), covering most of the area of interest, for each sample.

3 | RESULTS

3.1 | Patient characteristics

Six patients with verified nickel allergy were recruited to the study, all females, of ages 21-66 years (average 44 years). All patients developed clear, positive reactions against nickel at 96 hours after application of the nickel patch tests. One skin biopsy sample at 48 hours was removed due to processing failure.

3.2 | Nickel induces strong gene expression dynamics over time

Gene expression profiles were analyzed using microarrays from skin biopsies at baseline (indicated as 0 hours) as well as 2, 48, and 96 hours after nickel exposure. Differential gene expression analysis revealed 1554 (784 up/770 down; Table S1) and 3065 (1548 up/1517 down; Table S2) genes at 48 and 96 hours, respectively. We found no significant differentially expressed genes at 2 hours (Figure 1A). Visualization via a Venn diagram illustrated that the majority of differentially expressed genes (DEG) are shared between 48 and 96 hours, with 1347 uniquely DEGs at 96 hours (Figure 1B). These distinct gene expression profiles are represented in the PCA, displaying an overlap between 0- and 2-hour time points, with a clear separation between 48 and 96 hours (Figure 1C). In parallel, hierarchical clustering of the most significant DEGs over time evinced that 48 and 96 hours form unique and distinct clusters compared to 0 and 2 hours (Figure 1D).

3.3 | Nickel-induced allergic contact dermatitis causes leukocyte compositional changes

Allergic contact dermatitis involves the recruitment, activation, differentiation, and proliferation of various immune cells; therefore, we employed a leukocyte deconvolution algorithm on each individual sample over time. At baseline levels, resting mast cells and macrophage subsets were the predominant cell types observed, accounting for 50% of cells on average. Remaining leukocyte subsets were represented individually with mean fractions <10% (Figure 2A; Figure S1). Upon nickel exposure, significantly higher estimations of M1 macrophages, activated mast cells, neutrophils, activated NK cells, CD4+ memory T cells, and CD8+ T cells were observed, reaching a maximum peak at 48 hours (96 hours for CD8+ cells). Concomitantly, estimated numbers of M2 macrophages, resting mast cells, γΔ-T cells, and regulatory T cells (Treg) decreased significantly during the stimulation period, reaching lowest values after 48 and 96 hours (Figure 2B). Similarly, immunohistochemical staining of 48-hour-exposed skin biopsies revealed accumulation of CD8+ and CD68+ cells in nickel- and SLS-exposed skin (Figure S2).

3.4 | Time-course GSEA determines important gene sets in nickel contact allergy reaction

Nickel-induced ACD perturbs skin leukocyte composition over time, leading to the recruitment of different cellular subsets into the affected skin area. To unravel pivotal mechanisms from invading leukocytes, a time-course gene set enrichment analysis (GSEA) utilizing the GO Biological Processes database was applied to identify central gene sets with biological meaningful functions during nickel exposure. 1217 gene sets were positively, while 691 gene sets were negatively enriched with a FDR < 25%. Nodes with tight clustering, indicating high gene redundancy, involved immune responses (eg, leukocyte-mediated immunity, regulation of cell killing, T cell–mediated immunity, and NK cell–mediated immunity), T-cell activation, cell extravasation and migration, and cell cycle and DNA repair-associated gene sets (Figure 3). Additionally, gene sets for macrophage activation, cytokine production (IL-6, IL-8, IL-12, TNF superfamily, and IFN-γ), TH1/TH2 responses, apoptosis, mast cell activation, TLR pathway, and others were also enriched positively over time. The whole dataset is provided in Table S3. Top negatively enriched skin-related gene sets included keratinocyte proliferation and regulation of water loss via skin (Table S4).

3.5 | Enriched cell-related gene sets are associated with leukocyte composition estimations

To determine the relevance and linkage between the leukocyte composition estimates and enriched gene sets, gene set results

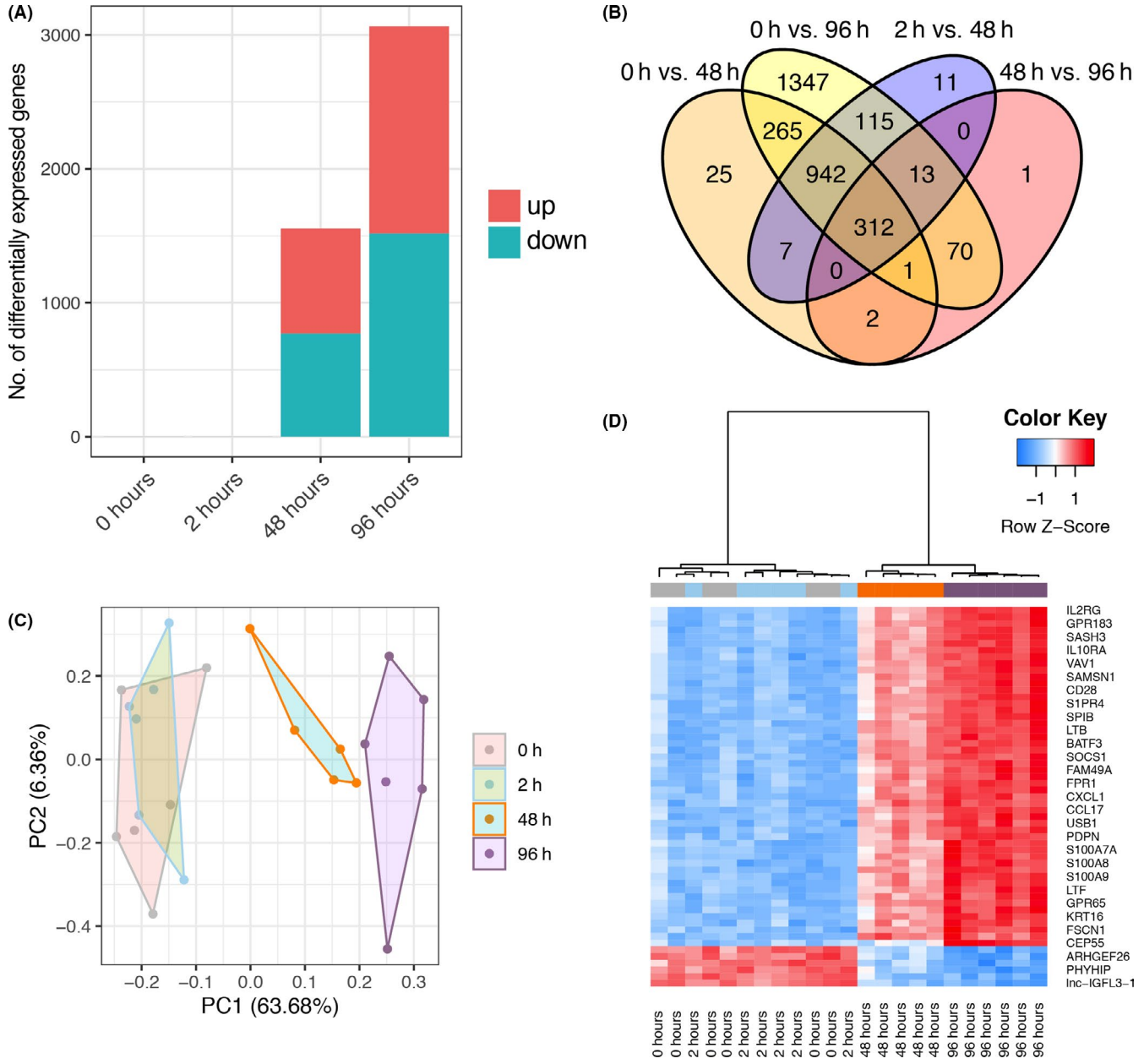

FIGURE 1 Differentially expressed genes (DEGs) over time during nickel-induced allergic contact dermatitis in human skin. Significantly up- (red) and downregulated (green) genes over time (A). Venn diagram representation to identify uniquely and shared DEGs between time point comparisons (B). Principal component (PC) analysis of gene expression profiles over time (C). Heatmap of highly significant DEGs across time points (D)

were filtered according to the highest rank at max metric, highest NES (>2.5), and a FDR < 0.001, resulting in a condensed table of 165 highly enriched gene sets. Within this dataset, responses involving T cells, B cells, macrophages, dendritic cells, neutrophils, and mast cells are highly enriched, which is in line with up-/downregulation of highlighted estimated leukocyte populations (Figure 2B). Cell-associated functional gene sets included IFN-γ response and signaling, cell killing and cytotoxicity, regulation and release of cytokines (IL-1β, IL-4, IL-10, IL-12, and IL-17), and extravasation and cellular chemotaxis (Table S3). Utilizing the annotation enrichment analysis tool EnrichR, the ARCHS4 Tissues database was used to decipher relevant cell types based on DEGs. Downregulated DEGs from 48 and 96 hours represented enrichment for "Skin (bulk tissue)," "Keratinocytes," and "Basal cells" without enrichment of any immune cell subsets. Contrary, upregulated DEGs displayed significant enrichment for immune cells including "Macrophage," "Natural Killer Cells," "Plasmacytoid Dendritic Cells," "CD4+ T Cell," "Regulatory T Cell," and "Dendritic Cell" without enrichment of skin-related cells. Additionally, we analyzed activation and differentiation markers of macrophage polarization based on previous findings.[31] *MMP12* and *SOCS3* were among the top upregulated DEGs as well as GSEA ranked genes (Table S5) at 48 and 96 hours.

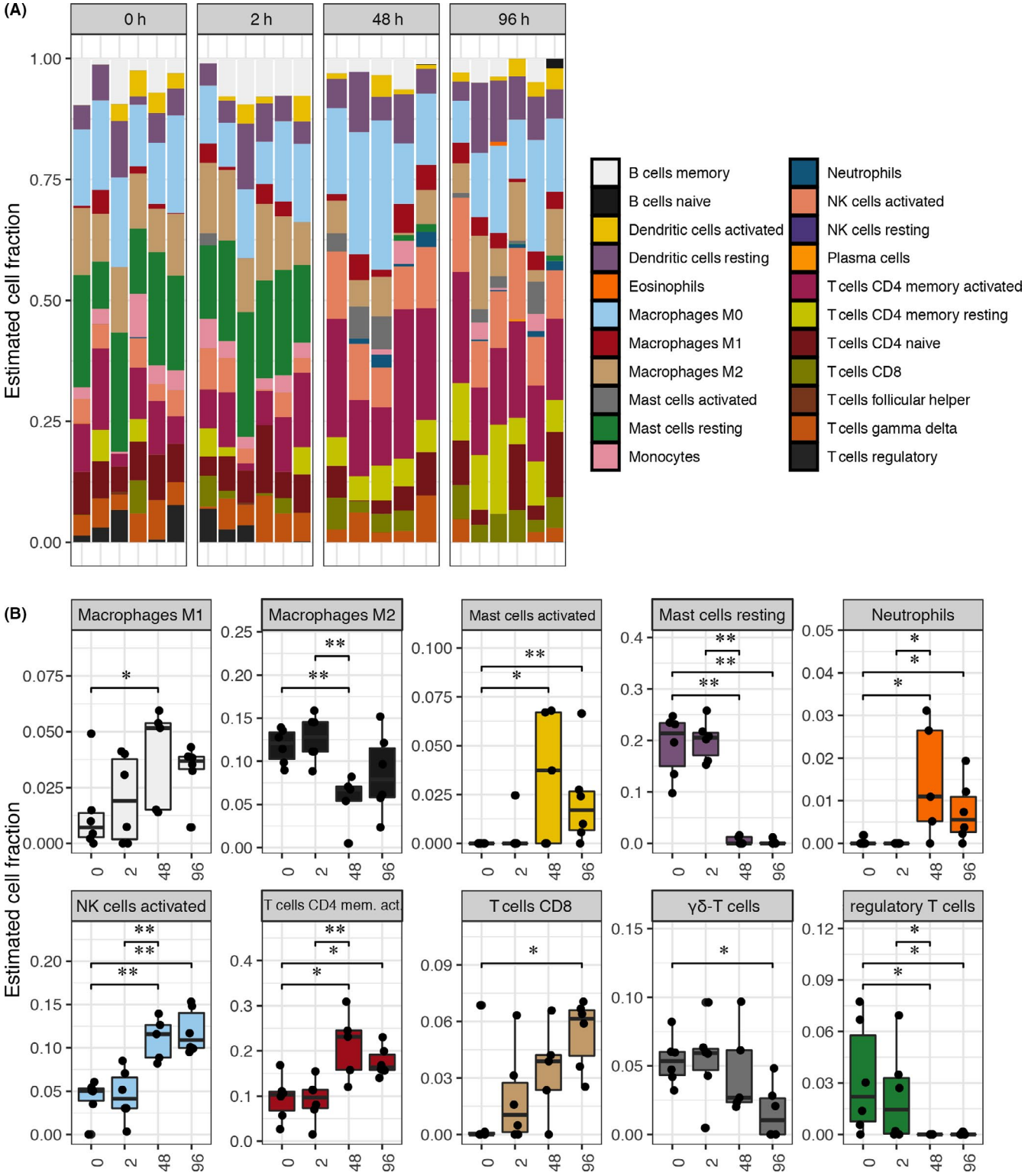

FIGURE 2 Nickel-induced contact allergy perturbates skin leukocyte composition. Estimated cell fractions from transcriptome-wide gene expression signatures, partitioned according to the investigated time point (A). Significantly changed cell populations over the allergen stimulation time course (B). $^{*}P < 0.05$, $^{**}P < 0.01$

Interestingly, *ARG1* was significantly downregulated at 48 hours, but *NOS2* displayed unchanged expression over time (Figure S3). The expression levels of *MMP12*, *SOCS3*, *ARG1*, and *NOS2* were validated by qPCR using technical replicates and an independent group of patients for biological validation (n = 7), confirming the findings from the microarrays (Figure S4).

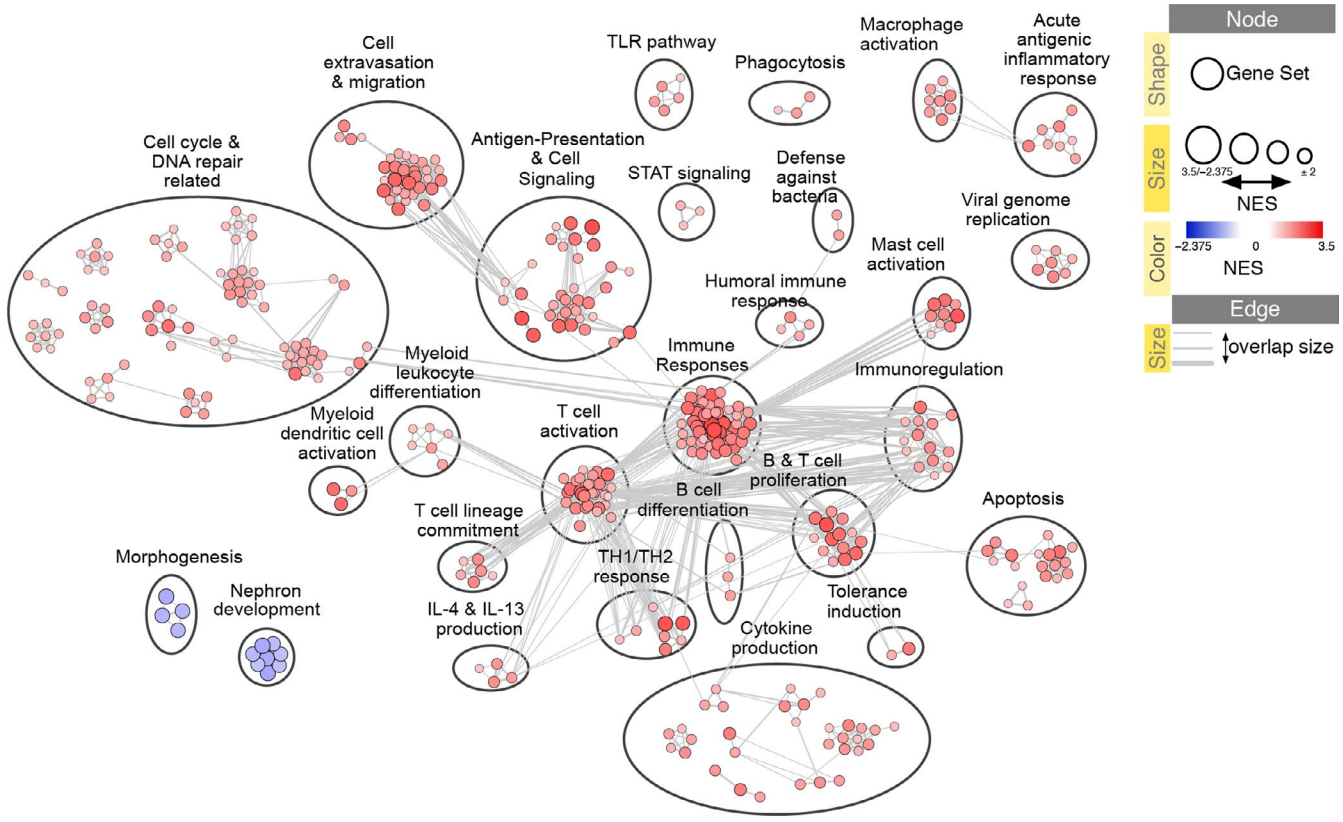

FIGURE 3 Time-course gene set enrichment analysis of skin biopsies after nickel exposure. Each node (circle) represents a gene set with either positive (red circles) or negative (blue circles) normalized enrichment score (NES). Edges link gene sets with overlapping genes. Only gene sets with an FDR < 0.01, $P < 0.05$, and NES < −2 and >2 were included in the visualization, and disconnected clusters <3 nodes were removed. Data were visualized with Cytoscape Enrichment Map

3.6 | Notch and interferon signaling pathways are highly enriched during nickel-induced contact allergy

To deepen our understanding of underlying pathways in nACD, we performed an additional time-course GSEA utilizing the Reactome database. 498 gene sets were positively, while 71 gene sets were negatively enriched over time with a FDR < 25%. Interferon signaling, including signaling of IFN-α/β/γ, as well as neutrophil degranulation and PD-1 signaling, was highly positively enriched (Figure 4A; Table S6). Contrary, Notch4 and Notch1-dependent signaling as well as keratinization were highly negatively enriched (Figure 4B; Table S7).

3.7 | Comparison of nickel and SLS skin exposure identifies NK cells as important cell subset in ACD

To point out relevant cellular subsets specific in nACD, we investigated the impact of SLS, a skin irritant, on leukocyte composition and induced immune reaction at 48 hours poststimulation. SLS skin irritation led to a significant change in gene expression profiles with 385 DEGs (274 up/111 down; Table S8). However, irritant stimulation resulted only in a small fraction of 16 uniquely DEGs compared to nickel with 1185 uniquely DEGs (Figure 5A). Unique SLS DEGs are enriched for skin-related biological processes, whereas unique nickel DEGs involve mainly T-cell activation and migration. Shared DEGs are mainly enriched for inflammatory responses, T-cell activation and responses, and cell migration (GO Biological Processes; Figure S5). Leukocyte deconvolution exhibited a significantly higher estimated fraction of neutrophils and NK cells in nACD compared to SLS-induced ICD (Figure 5B, whole dataset Figure S6). Next, we performed KEGG pathway enrichment analysis to unravel unique functional themes between DEGs from nickel and SLS stimulation. We revealed 14 unique pathways in the nickel samples, including "JAK-STAT signaling," "Natural killer cell mediated cytotoxicity," and "T cell receptor signaling pathway." In SLS, "TNF signaling pathway" was uniquely enriched (Figure 5C).

3.8 | In-depth analysis of NK cell–related pathways

The higher estimated NK cell counts as well as functional enrichment highlight a potential role of NK cells in nACD. To deepen our insights, the KEGG pathway "Natural killer cell mediated cytotoxicity" was analyzed to study the NK cell involvement in more detail. The pathway was enriched of 29 DEGs, all of being upregulated at 48-hour nACD (Figure S7). Essential key genes in this pathway included *KLRD1*, *ITGAL*, *GZMB*, and *FASLG* (Figure 6A). Additionally,

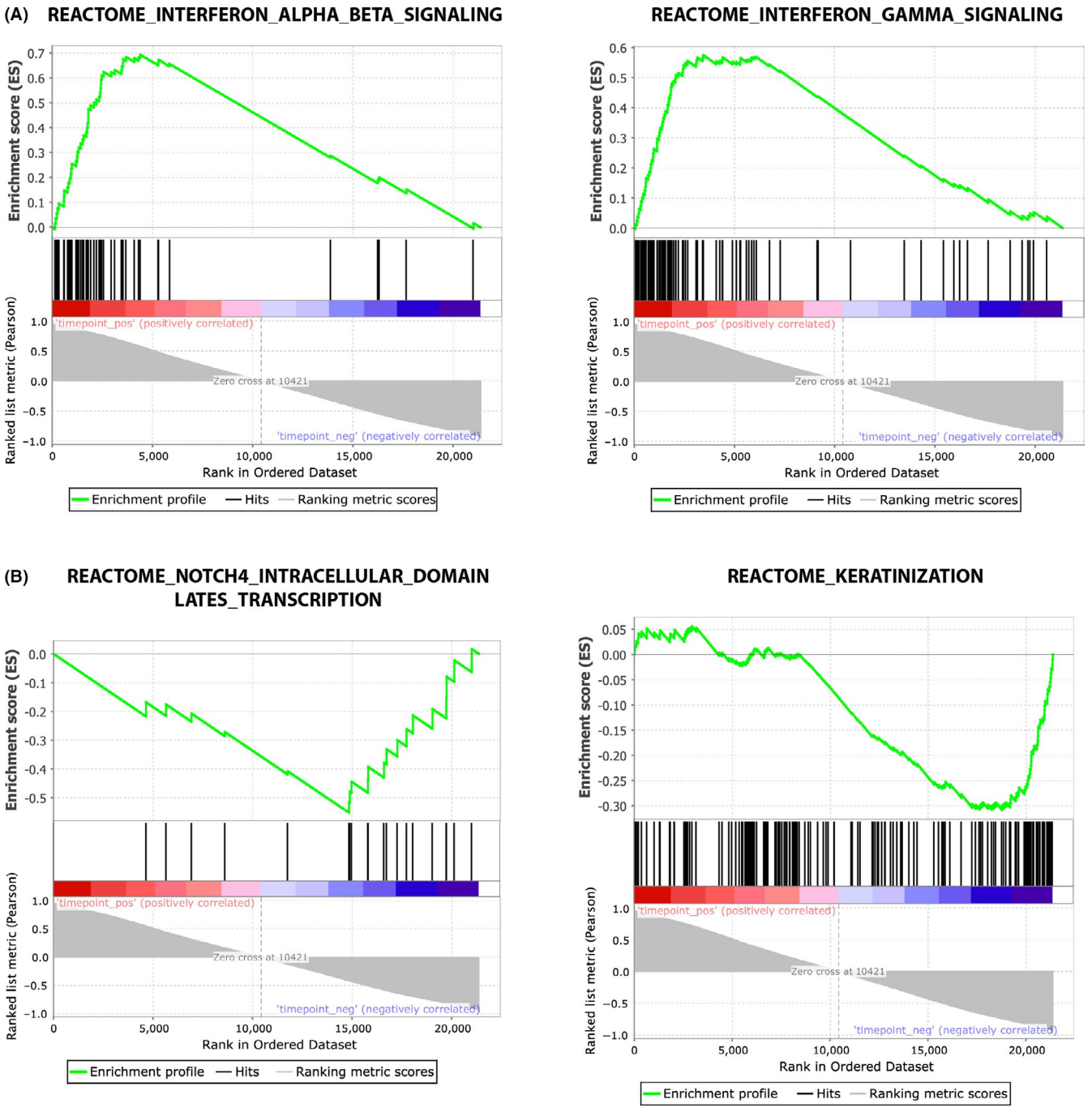

FIGURE 4 Time-course GSEA result using the Reactome database. Selected highly enriched ($P < .01$, FDR < 0.05) pathways which are positively (A) and negatively (B) enriched over time course. The *x*-axis depicts genes represented in gene sets as the *y*-axis represents the enrichment score (ES). ES represents the degree of over-representation of a gene set at the top or bottom of the ranked gene list. The colored band under the *x*-axis represents the correlation of genes with time points (red = later time points, blue = early time points)

the KEGG pathway "JAK-STAT signaling" was enriched with 38 DEGs. Furthermore, the Reactome database was used to identify additional enriched immunological pathways. Reactome analysis uncovered interferon signaling and interferon gamma as highly enriched pathways in nACD. Further highly enriched key pathways included signaling by interleukins, neutrophil degranulation, extracellular matrix organization, keratinization, and IL-4 and IL-13 signaling (Figure 6B).

4 | DISCUSSION

Time-course gene expression analysis revealed novel dynamics in the immune cell flux as well as related immune pathways in human skin during nACD. Our study provides novel, data-driven, circumscribed cellular targets with associated pathways for deeper mechanistic studies in nickel contact dermatitis, the most common contact allergen in industrialized countries.[2]

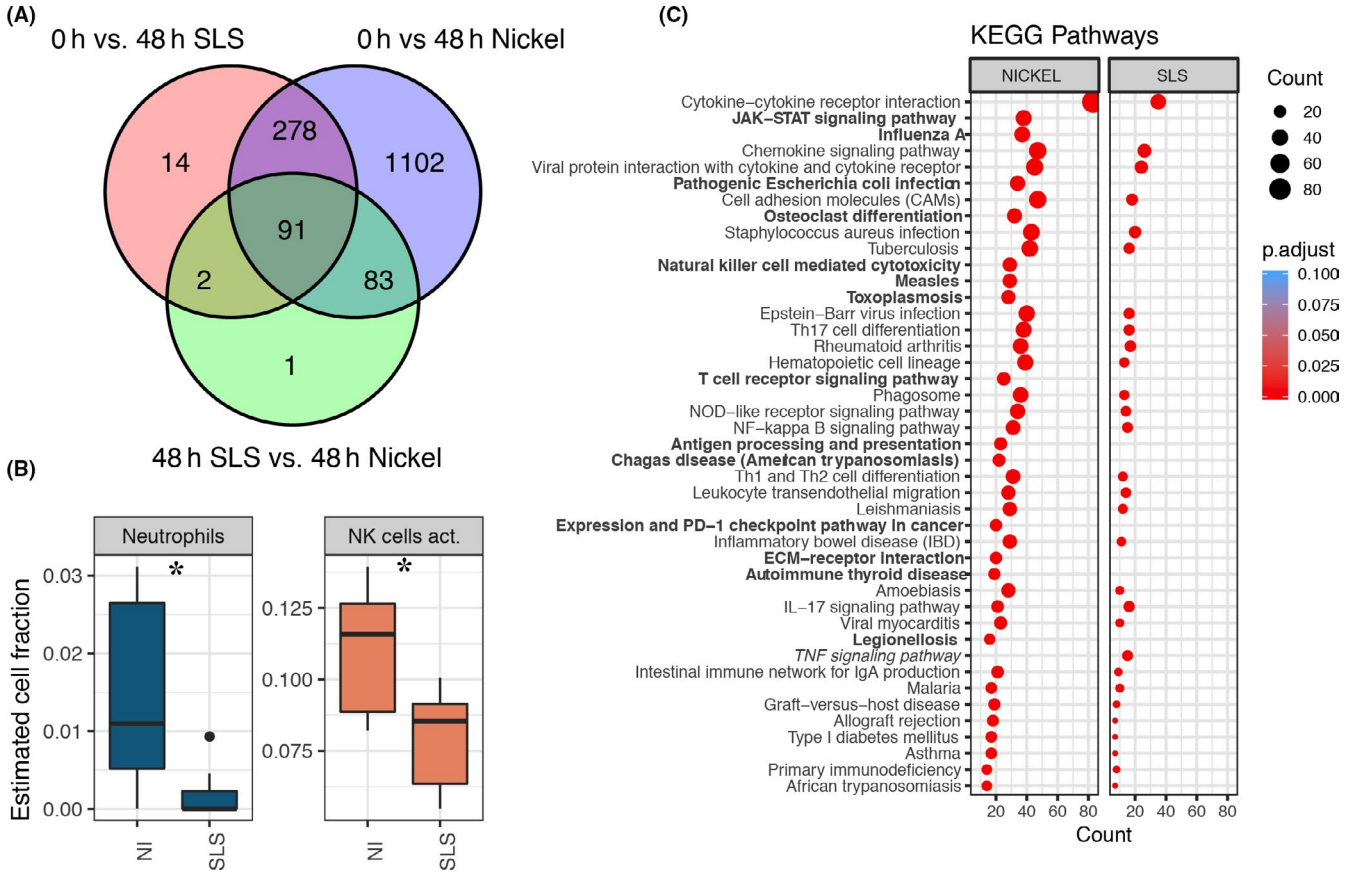

FIGURE 5 Analysis of nickel vs sodium lauryl sulfate (SLS) skin exposure at 48 h. Venn diagram representation to identify uniquely and shared differentially expressed genes between nickel and SLS comparisons (A). The CIBERSORT algorithm was used to identify different cell subsets after nickel and SLS exposure after 48 h (B). KEGG pathway enrichment analysis was conducted using clusterProfiler. Uniquely enriched pathways in nickel exposure are highlighted in bold text, whereas uniquely enriched pathways in SLS are highlighted in oblique text (C). *$P < 0.05$

During the elicitation phase, re-entered nickel ions bind directly to MHC complexes as well as are taken up by dendritic cells leading to activation of skin-resident memory T cells as well as to migration of memory T cells into the skin.[32] Memory T cells are known central players in ACD, initiating the inflammatory cascade, and furthermore trigger the recruitment of immune cells into inflamed tissue.[33] Since the involvement of memory T cells is well described, we aimed to unravel enigmatic roles of further involved cell types.[34] In the early response phase, represented at the 2-hour time point, leukocyte composition did not differ significantly compared to unaffected skin. The result is in line with a previous study showing no induction of associated genes by nickel at early time points.[35] We identified significant changes in estimated immune cell fractions during late-phase (48-96 hours) nickel challenge, dominated by influx and/or activation of memory T cells, cytotoxic cells (NK cells, CD8+ T cells), mast cells, and M1-polarized macrophages.

Recent mice data suggest that splenic NK cells are activated during nickel challenge in a NKG2D-dependent fashion.[36] Moreover, mice NK cells display the capability to maintain a persistent, hapten-specific immune memory.[37] Although human data concerning these mechanistic insights are missing, ACD patients display a significant higher number of NK cell infiltrates in affected skin.[38,39] Thus, activated NK cell might amplify the immune reaction via secretion of IFN-γ, additionally activating dendritic cells, which leads to enhanced T-cell responses. Furthermore, nickel-specific CD4+ and CD8+ T cells have been described in nickel-allergic patients being capable to produce IFN-γ and granzyme B.[40] Earlier studies suggest that CD8+ T cells selectively kill human IFN-γ-primed keratinocytes, rendering them prone toward T_H1-dependent cytotoxicity.[41] Those findings are underlined by our time-course GSEA. We identified highly enriched gene sets (Table S3) related to cytotoxicity including IFN-γ signaling and NK cell–mediated cytotoxicity. Contrary, gene sets concerning epithelial development, skin integrity, and keratinocyte proliferation are highly negatively enriched. Asserting the robustness of our results, cytotoxic-mediated cellular damage seems to play a major role in the acute phase of nACD. To strengthen our hypothesis that these mechanisms are essential in ACD, we compared nACD with SLS-induced ICD. The latter arises from chemical and physical stimuli releasing pro-inflammatory mediators and, therefore, results in skin barrier disruption, epidermal damage, and inflammation.[42,43] Irritant compounds are able to directly activate innate immune mechanisms, which in turn attract nonspecific T

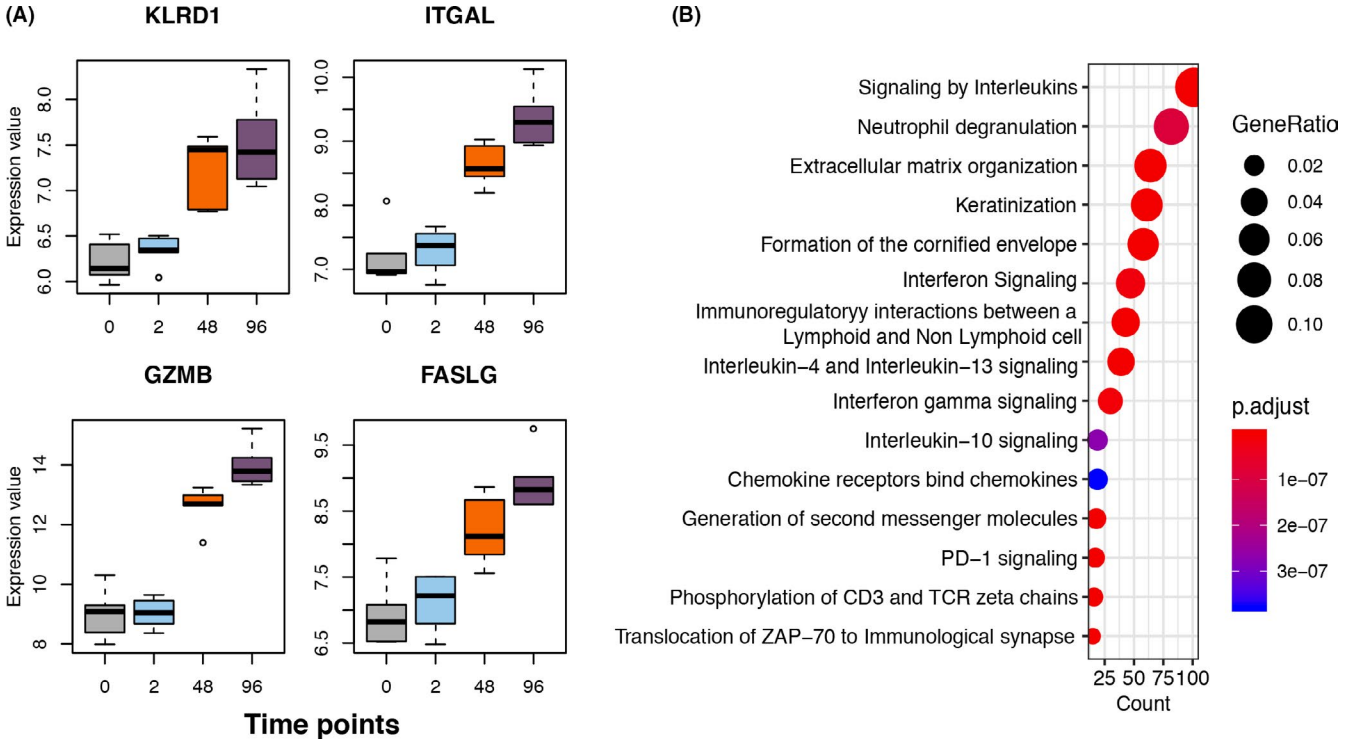

FIGURE 6 Natural killer cell and cytotoxicity-associated genes identified in KEGG pathway analysis. Expression of single essential NK cell–mediated cytotoxicity genes over time (A). Reactome pathway analysis of differentially expressed genes at 48 h of nickel stimulation (B)

cells.[44] Hence, dissimilar initial mechanisms might trigger different immune cell subsets. We discovered that activated NK cells were uniquely upregulated in nACD, highlighting the importance of this cellular subset.

The involvement of IFN-γ and associated pathways might explain the bias toward M1 macrophage polarization found in our study cohort. Macrophages are subgrouped by two antagonistic arginine metabolic pathways: iNOS representing M1-like (pro-inflammatory), and Arg1 representing M2-like macrophage (anti-inflammatory) phenotypes.[45] Thus, the induced pro-inflammatory skin milieu leads to M1 polarization, triggering higher iNOS expression which is worsening contact dermatitis.[46] However, we observed a relatively high fraction (10%-15%) of M2 macrophages at baseline levels compared to M1 macrophages. Although well known for the suppression of T_H1 responses and tissue repair properties, M2 macrophages might exacerbate contact dermatitis via the secretion of CXCL2[47] and matrix metalloproteinase 12 (MMP12).[48,49] Although MMP12 was linked with tissue-remodeling processes, this enzyme exhibits an essential role in cellular recruitment via the induction of chemokines.[50-52] Our data suggest a potential link of the described mouse data in human skin, as *MMP12* and *SOCS3* are highly upregulated and enriched in our analysis.

Mast cells appear to elicit a dual role in contact dermatitis; first they seem to promote inflammation (eg, boosting antigenicity of haptens, activation of hapten-specific IgM, and complement activation), followed by inhibitory immune mechanism and limitation of tissue injury.[53-55] In our study, mast cell kinetics displayed highest value of activated cells at 48 hours, concomitantly with neutrophils. GSEA revealed highly positive enrichment of mast cell activation-related gene sets over time. However, the importance of mast cell during contact dermatitis is still controversial.[56-59] Recently, transgenic mice study revealed that mast cell activation is required for induction of contact dermatitis, but merely needed for dermatitis resolution.[53] Nonetheless, detailed insights into human mast cell biology during contact dermatitis are scarce.

Lastly, we observed negative kinetics of estimated numbers of Tregs and γΔ T cells over time. The role of human epidermal γΔ T cells in nACD is barely investigated, but earlier conducted mouse studies suggest that this cell population may suppress contact dermatitis.[60,61] Moreover, Tregs appear to play a pivotal role in immune regulation during nickel allergy with altered functional profiles. Tregs from nickel-allergic patients demonstrate limited capacity to suppress nickel-specific effector T cells. In contrast, Tregs from healthy probands showed strong regulatory properties in a cell contact–dependent manner.[62,63] GSEA revealed a highly negative enrichment of Notch1 and Notch4 signaling during nACD. Notch signaling is an evolutionally highly conserved pathway, significantly regulating cell fate as well as T-cell differentiation and function.[64-66] Since this pathway is involved in epidermal processes and Treg function, it is not possible for us to determine the involvement of this pathway specifically on Tregs. Nevertheless, Notch signaling seems to be a major pathway in other skin diseases such as atopic dermatitis.[67]

In summary, we comprehensively profiled nickel-induced transcriptomic changes over time. Utilizing an integrative and

data-driven approach, we identified major leukocyte compositional changes, biological processes, and pathways associated with ACD. Our findings confirm previous findings, but also highlight novel associated cellular and gene expression changes not shown in humans before. Thus, our findings serve as a useful basis, indicating target cell population and genes, to further elucidate the underlying mechanisms of ACD, with the potential to unravel new treatment strategies.

ACKNOWLEDGMENTS

We thank all patients who participated in our study.

CONFLICT OF INTEREST

Dr Wisgrill, Werner, Dr Lehto, Dr Berger, Dr Lauerma, Dr Alenius, and Dr Fyhrquist have nothing to disclosure.

AUTHOR CONTRIBUTIONS

EL, AL, HA, and NF planned, performed, and analyzed the experiments. HA, AL, AB, and NF contributed to discussions. LW, PW, AB, HA, and NF interpreted the data and wrote the manuscript.

ORCID

Lukas Wisgrill https://orcid.org/0000-0001-9833-9499
Paulina Werner https://orcid.org/0000-0002-8112-0252
Erja Jalonen https://orcid.org/0000-0002-0434-8851
Antti Lauerma https://orcid.org/0000-0002-5078-3547
Harri Alenius https://orcid.org/0000-0003-0106-8923
Nanna Fyhrquist https://orcid.org/0000-0002-5408-0005

REFERENCES

1. Thyssen JP, Johansen JD, Menne T, Nielsen NH, Linneberg A. Nickel allergy in Danish women before and after nickel regulation. *N Engl J Med*. 2009;360(21):2259-2260.
2. Cutler CP. Use of metals in our society. In: Jennifer K, Chen JPT, eds. *Metal Allergy*. 1st edn. Cham, Switzerland: Springer International Publishing; 2018:3-16.
3. Diepgen TL, Ofenloch RF, Bruze M, et al. Prevalence of contact allergy in the general population in different European regions. *Br J Dermatol*. 2016;174(2):319-329.
4. Fors R, Persson M, Bergstrom E, Stenlund H, Stymne B, Stenberg B. Nickel allergy–prevalence in a population of Swedish youths from patch test and questionnaire data. *Contact Dermatitis*. 2008;58(2):80-87.
5. Lagrelius M, Wahlgren CF, Matura M, Kull I, Liden C. High prevalence of contact allergy in adolescence: results from the population-based BAMSE birth cohort. *Contact Dermatitis*. 2016;74(1):44-51.
6. Lidén C. Metal allergy: nickel. In: Jennifer K, Chen JP, eds. *Metal allergy*. 1st edn. Cham, Switzerland: Springer International Publishing; 2018:423-434.
7. Ahlstrom MG, Thyssen JP, Wennervaldt M, Menne T, Johansen JD. Nickel allergy and allergic contact dermatitis: a clinical review of immunology, epidemiology, exposure, and treatment. *Contact Dermatitis*. 2019;81(4):227-241.
8. Julander A, Midander K, Herting G, et al. New UK nickel-plated steel coins constitute an increased allergy and eczema risk. *Contact Dermatitis*. 2013;68(6):323-330.
9. Midander K, Hurtig A, Borg Tornberg A, Julander A. Allergy risks with laptop computers – nickel and cobalt release. *Contact Dermatitis*. 2016;74(6):353-359.
10. Thyssen JP, Milting K, Bregnhoj A, Sosted H, Duus Johansen J, Menne T. Nickel allergy in patch-tested female hairdressers and assessment of nickel release from hairdressers' scissors and crochet hooks. *Contact Dermatitis*. 2009;61(5):281-286.
11. Kaplan DH, Igyarto BZ, Gaspari AA. Early immune events in the induction of allergic contact dermatitis. *Nat Rev Immunol*. 2012;12(2):114-124.
12. Martin SF. New concepts in cutaneous allergy. *Contact Dermatitis*. 2015;72(1):2-10.
13. Schmidt JD, Ahlstrom MG, Johansen JD, et al. Rapid allergen-induced interleukin-17 and interferon-gamma secretion by skin-resident memory CD8(+) T cells. *Contact Dermatitis*. 2017;76(4):218-227.
14. Uter W, Werfel T, White IR, Johansen JD. Contact allergy: a review of current problems from a clinical perspective. *Int J Environ Res Public Health*. 2018;15(6):1108.
15. Marwah VS, Scala G, Kinaret PAS, et al. eUTOPIA: solUTion for omics data preprocessing and analysis. *Source Code Biol Med*. 2019;14:1.
16. Johnson WE, Li C, Rabinovic A. Adjusting batch effects in microarray expression data using empirical Bayes methods. *Biostatistics*. 2007;8(1):118-127.
17. Ritchie ME, Phipson B, Wu DI, et al. limma powers differential expression analyses for RNA-sequencing and microarray studies. *Nucleic Acids Res*. 2015;43(7):e47. https://doi.org/10.1093/nar/gkv007
18. Newman AM, Liu CL, Green MR, et al. Robust enumeration of cell subsets from tissue expression profiles. *Nat Methods*. 2015;12(5):453-457.
19. Subramanian A, Kuehn H, Gould J, Tamayo P, Mesirov JP. GSEA-P: a desktop application for Gene Set Enrichment Analysis. *Bioinformatics* 2007;23(23):3251-3253.
20. Subramanian A, Tamayo P, Mootha VK, et al. Gene set enrichment analysis: a knowledge-based approach for interpreting genome-wide expression profiles. *Proc Natl Acad Sci USA*. 2005;102(43):15545-15550.
21. Merico D, Isserlin R, Stueker O, Emili A, Bader GD. Enrichment map: a network-based method for gene-set enrichment visualization and interpretation. *PLoS One*. 2010;5(11):e13984.
22. Cline MS, Smoot M, Cerami E, et al. Integration of biological networks and gene expression data using Cytoscape. *Nat Protoc*. 2007;2(10):2366-2382.
23. Oesper L, Merico D, Isserlin R, Bader GD. WordCloud: a Cytoscape plugin to create a visual semantic summary of networks. *Source Code Biol Med*. 2011;6:7.
24. Wickham H. *ggplot2: Elegant Graphics for Data Analysis*. 1st edn. New York, NY: Springer-Verlag; 2009.
25. Kassambara. ggpubr: 'ggplot2' Based Publication Ready Plots. 2019. https://github.com/kassambara/ggpubr. Accessed November 25, 2019.
26. Tang Y, Horikoshi M, Li W. ggfortify: unified interface to visualize statistical results of popular R packages. *The R Journal* 2016;8(2):474.
27. Chen H. VennDiagram: Generate High-Resolution Venn and Euler Plots. 2018. https://rdrr.io/cran/VennDiagram/
28. Yu G, Wang LG, Han Y, He QY. clusterProfiler: an R package for comparing biological themes among gene clusters. *OMICS*. 2012;16(5):284-287.
29. Yu G, He QY. ReactomePA: an R/Bioconductor package for reactome pathway analysis and visualization. *Mol Biosyst*. 2016;12(2):477-479.
30. Luo W, Brouwer C. Pathview: an R/Bioconductor package for pathway-based data integration and visualization. *Bioinformatics* 2013;29(14):1830-1831.

31. Suzuki K, Meguro K, Nakagomi D, Nakajima H. Roles of alternatively activated M2 macrophages in allergic contact dermatitis. *Allergol Int*. 2017;66(3):392-397.
32. Schmidt M, Goebeler M. Immunology of metal allergies. *J Dtsch Dermatol Ges*. 2015;13(7):653-660.
33. Nourshargh S, Alon R. Leukocyte migration into inflamed tissues. *Immunity* 2014;41(5):694-707.
34. Meller S, Lauerma AI, Kopp FM, et al. Chemokine responses distinguish chemical-induced allergic from irritant skin inflammation: memory T cells make the difference. *J Allergy Clin Immunol*. 2007;119(6):1470-1480.
35. Pedersen MB, Skov L, Menne T, Johansen JD, Olsen J. Gene expression time course in the human skin during elicitation of allergic contact dermatitis. *J Invest Dermatol*. 2007;127(11):2585-2595.
36. Kim JY, Huh K, Lee KY, Yang JM, Kim TJ. Nickel induces secretion of IFN-gamma by splenic natural killer cells. *Exp Mol Med*. 2009;41(4):288-295.
37. O'Leary JG, Goodarzi M, Drayton DL, von Andrian UH. T cell- and B cell-independent adaptive immunity mediated by natural killer cells. *Nat Immunol*. 2006;7(5):507-516.
38. Carbone T, Nasorri F, Pennino D, et al. CD56highCD16-CD62L- NK cells accumulate in allergic contact dermatitis and contribute to the expression of allergic responses. *J Immunol*. 2010;184(2):1102-1110.
39. von Bubnoff D, Andres E, Hentges F, Bieber T, Michel T, Zimmer J. Natural killer cells in atopic and autoimmune diseases of the skin. *J Allergy Clin Immunol*. 2010;125(1):60-68.
40. Bechara R, Pollastro S, Azoury ME, et al. Identification and characterization of circulating naive CD4+ and CD8+ T cells recognizing nickel. *Front Immunol*. 2019;10:1331.
41. Traidl C, Sebastiani S, Albanesi C, et al. Disparate cytotoxic activity of nickel-specific CD8+ and CD4+ T cell subsets against keratinocytes. *J Immunol*. 2000;165(6):3058-3064.
42. Berardesca E, Distante F. Mechanisms of skin irritations. *Curr Probl Dermatol*. 1995;23:1-8.
43. Mathias CG, Maibach HI. Dermatotoxicology monographs I. Cutaneous irritation: factors influencing the response to irritants. *Clin Toxicol*. 1978;13(3):333-346.
44. Gober MD, Gaspari AA. Allergic contact dermatitis. *Curr Dir Autoimmun*. 2008;10:1-26.
45. Orecchioni M, Ghosheh Y, Pramod AB, Ley K. Macrophage polarization: different gene signatures in M1(LPS+) vs. classically and M2(LPS-) vs. Alternatively Activated Macrophages. *Front Immunol*. 2019;10:1084.
46. Suwanpradid J, Shih M, Pontius L, et al. Arginase1 deficiency in monocytes/macrophages upregulates inducible nitric oxide synthase to promote cutaneous contact hypersensitivity. *J Immunol*. 2017;199(5):1827-1834.
47. Natsuaki Y, Egawa G, Nakamizo S, et al. Perivascular leukocyte clusters are essential for efficient activation of effector T cells in the skin. *Nat Immunol*. 2014;15(11):1064-1069.
48. Hartmann B, Staedtler F, Hartmann N, Meingassner J, Firat H. Gene expression profiling of skin and draining lymph nodes of rats affected with cutaneous contact hypersensitivity. *Inflamm Res*. 2006;55(8):322-334.
49. Nakagomi D, Suzuki K, Meguro K, et al. Matrix metalloproteinase 12 is produced by M2 macrophages and plays important roles in the development of contact hypersensitivity. *J Allergy Clin Immunol*. 2015;135(5):1397-1400.
50. Dean RA, Cox JH, Bellac CL, Doucet A, Starr AE, Overall CM. Macrophage-specific metalloelastase (MMP-12) truncates and inactivates ELR+ CXC chemokines and generates CCL2, -7, -8, and -13 antagonists: potential role of the macrophage in terminating polymorphonuclear leukocyte influx. *Blood* 2008;112(8):3455-3464.
51. Nénan S, Boichot E, Planquois J-M, et al. Effects of depletion of neutrophils or macrophages on the inflammatory response induced by metalloelastase (MMP-12) in mice airways. *Eur J Pharmacol*. 2008;579(1-3):374-381.
52. Senior RM, Griffin GL, Mecham RP. Chemotactic responses of fibroblasts to tropoelastin and elastin-derived peptides. *J Clin Invest*. 1982;70(3):614-618.
53. Dudeck A, Dudeck J, Scholten J, et al. Mast cells are key promoters of contact allergy that mediate the adjuvant effects of haptens. *Immunity* 2011;34(6):973-984.
54. Gaudenzio N, Marichal T, Galli SJ, Reber LL. Genetic and imaging approaches reveal pro-inflammatory and immunoregulatory roles of mast cells in contact hypersensitivity. *Front Immunol*. 2018;9:1275.
55. Gimenez-Rivera VA, Siebenhaar F, Zimmermann C, Siiskonen H, Metz M, Maurer M. Mast cells limit the exacerbation of chronic allergic contact dermatitis in response to repeated allergen exposure. *J Immunol*. 2016;197(11):4240-4246.
56. Galli SJ, Hammel I. Unequivocal delayed hypersensitivity in mast cell-deficient and beige mice. *Science* 1984;226(4675):710-713.
57. Grimbaldeston MA, Nakae S, Kalesnikoff J, Tsai M, Galli SJ. Mast cell-derived interleukin 10 limits skin pathology in contact dermatitis and chronic irradiation with ultraviolet B. *Nat Immunol*. 2007;8(10):1095-1104.
58. McLachlan JB, Catron DM, Moon JJ, Jenkins MK. Dendritic cell antigen presentation drives simultaneous cytokine production by effector and regulatory T cells in inflamed skin. *Immunity* 2009;30(2):277-288.
59. Tsuji RF, Szczepanik M, Kawikova I, et al. B cell-dependent T cell responses: IgM antibodies are required to elicit contact sensitivity. *J Exp Med*. 2002;196(10):1277-1290.
60. Lewis JM, Girardi M, Roberts SJ, Barbee SD, Hayday AC, Tigelaar RE. Selection of the cutaneous intraepithelial gammadelta+ T cell repertoire by a thymic stromal determinant. *Nat Immunol*. 2006;7(8):843-850.
61. Toulon A, Breton L, Taylor KR, et al. A role for human skin-resident T cells in wound healing. *J Exp Med*. 2009;206(4):743-750.
62. Cavani A, Nasorri F, Ottaviani C, Sebastiani S, De Pita O, Girolomoni G. Human CD25+ regulatory T cells maintain immune tolerance to nickel in healthy, nonallergic individuals. *J Immunol*. 2003;171(11):5760-5768.
63. Trzonkowski P, Szmit E, Mysliwska J, Dobyszuk A, Mysliwski A. CD4+CD25+ T regulatory cells inhibit cytotoxic activity of T CD8+ and NK lymphocytes in the direct cell-to-cell interaction. *Clin Immunol*. 2004;112(3):258-267.
64. Amsen D, Blander JM, Lee GR, Tanigaki K, Honjo T, Flavell RA. Instruction of distinct CD4 T helper cell fates by different notch ligands on antigen-presenting cells. *Cell*. 2004;117(4):515-526.
65. Massi D, Panelos J. Notch signaling and the developing skin epidermis. *Adv Exp Med Biol*. 2012;727:131-141.
66. Tu LiLi, Fang TC, Artis D, et al. Notch signaling is an important regulator of type 2 immunity. *J Exp Med*. 2005;202(8):1037-1042.
67. Melnik BC. The potential role of impaired Notch signalling in atopic dermatitis. *Acta Derm Venereol*. 2015;95(1):5-11.

SUPPORTING INFORMATION

Additional supporting information may be found online in the Supporting Information section.

How to cite this article: Wisgrill L, Werner P, Jalonen E, et al. Integrative transcriptome analysis deciphers mechanisms of nickel contact dermatitis. *Allergy*. 2021;76:804–815. https://doi.org/10.1111/all.14519